

The metal abundance distribution of the oldest stellar component in the Sculptor dwarf spheroidal galaxy^{*}

G. Clementini¹†, V. Ripepi², A. Bragaglia¹, A.F. Martinez Fiorenzano^{3,4},
E.V. Held³, and R.G. Gratton³

¹*INAF - Osservatorio Astronomico di Bologna, via Ranzani 1, I-40127 Bologna, Italy*

²*INAF - Osservatorio Astronomico di Capodimonte, via Moiarello 16, I-80131 Napoli, Italy*

³*INAF - Osservatorio Astronomico di Padova, vicolo dell'Osservatorio 5, I-35122 Padova, Italy*

⁴*Dipartimento di Astronomia, Università di Padova, vicolo dell'Osservatorio 2, I-35122 Padova, Italy*

Received 2005 ; in original form 2005

ABSTRACT

Low resolution spectroscopy obtained with FORS2 at the Very Large Telescope (VLT) has been used to measure individual metal abundances ($[\text{Fe}/\text{H}]$) for 110 variable stars, including 107 RR Lyrae stars and 1 Anomalous Cepheid, and trace the metal distribution of the oldest stellar component in the Sculptor dwarf spheroidal galaxy. The RR Lyrae stars are spread over a $15' \times 15'$ area around the galaxy centre. Their metallicities have an average value of $[\text{Fe}/\text{H}] = -1.83 \pm 0.03$ (r.m.s. 0.26 dex) and cover the metallicity range $-2.40 < [\text{Fe}/\text{H}] < -0.85$ (on the scale of Zinn & West 1984), but there is only one variable having $[\text{Fe}/\text{H}] > -1.3$. The star-to-star scatter is larger than typical errors on individual metallicities ($\pm 0.15 - 0.16$ dex), indicating a real spread in metal abundances. The radial velocities measured from the RR Lyrae spectra have a dispersion of 12.9 km s^{-1} . This value is consistent with the dispersion derived by Tolstoy et al. (2004) for metal-poor red giants associated to the blue horizontal branch stars in Sculptor. Along with the metallicity distribution these results suggest that most of the RR Lyrae stars in Sculptor arise from the same burst of stellar formation that produced the metal-poor component giving origin to the galaxy blue horizontal branch. The metal-rich red horizontal branch population found to be centrally concentrated only produced a few (if any) of the RR Lyrae stars in our sample. The spectroscopic metallicities were used along with the apparent luminosities to study the luminosity-metallicity relation followed by the RR Lyrae stars in Sculptor, for which we derive a shallow slope of 0.09 mag/dex. This result can be due to a high level of evolution off the zero age horizontal branch of the RR Lyrae stars in this galaxy, again in agreement with their origin from the blue horizontal branch population.

Key words: stars: abundances – stars: evolution – stars: Population II – stars: variables: other – galaxies: individual: Sculptor dwarf Spheroidal

1 INTRODUCTION

In hierarchical merging scenarios dwarf galaxies are thought to be the bricks from which larger galaxies were assembled. The study of the star formation history (SFH) and of

the chemical evolution of presently existing dwarf galaxies is then extremely important for a proper understanding of the formation and evolution of the larger systems that this type of galaxies may have contributed to build in the past. Colour magnitude diagrams (CMDs) reaching the faint main sequence turn-off (TO) of the oldest stellar components are the most traditional and reliable way to derive the SFH of any individual dwarf galaxy. However, these detailed studies, possible so far mainly for the dwarf members of the Local Group (LG), require very time consuming observations. The RR Lyrae variables, being about 3 magnitudes

^{*} Based on data collected at the European Southern Observatory, proposal number 71.B-0621

† E-mail: gisella.clementini@bo.astro.it; ripepi@na.astro.it;
angela.bragaglia@bo.astro.it; fiorenzano@pd.astro.it;
held@pd.astro.it; gratton@pd.astro.it

brighter than coeval TO stars ($t > 10$ Gyrs), are much easier to observe. They offer an excellent tool for tracing the oldest stellar populations, and therefore the epoch of galaxy formation, in composite systems such as the resolved LG dwarf galaxies. Recent work by several groups has led to the discovery of RR Lyrae stars in increasing numbers of LG dwarf galaxies (e.g. Leo I and II, IC 1613, Fornax, And VI, NGC6822: Held et al. 2001; Siegel & Majewski 2000; Dolphin et al. 2001; Bersier & Wood 2002; Pritzl et al. 2002; Clementini et al. 2003a, just to mention a few of them). An early stellar population, nearly coeval to the old Galactic globular clusters, has been found in the majority of LG galaxies, irrespective of their star formation histories. This indicates that all LG dwarfs started forming stars at an early epoch, ~ 13 Gyr ago (e.g. Held et al. 2000).

The Sculptor dwarf spheroidal galaxy is no exception to this general trend. 226 RR Lyrae stars and 3 Anomalous Cepheids have been detected in a $15' \times 15'$ area around the galaxy centre by Kaluzny et al. (1995) who published multi-epoch photometry for all of them. Kaluzny et al. (1995) also found that the period distribution of the RRAb stars shows a sharp cut-off at $P = 0.475$ d implying a metallicity of $[\text{Fe}/\text{H}] \leq -1.7$ (on the Zinn & West 1984 scale), and that the dispersion of the average V magnitudes is most likely due to the metallicity spread exhibited by the stars in this galaxy. Similarly, Kovács (2001) found $\langle [\text{Fe}/\text{H}] \rangle \sim -1.5$ with a large dispersion from about -2.0 to -0.8 dex (on the metallicity scale by Jurcsik 1995), from the Fourier decomposition of the light curves of the RRAb stars.

Indeed, Sculptor dwarf spheroidal (dSph) has long been known, from photometric studies, to have a large metallicity spread and bimodality in the metallicity and spatial distribution of its horizontal branch (HB) stars (Majewski et al. 1999; Hurley-Keller et al. 1999; Harbeck et al. 2001; Rizzi et al. 2004; Babusiaux et al. 2005). Very few spectroscopic determinations of the metal abundance of Sculptor stars existed so far (Norris & Bessell 1998; Tolstoy et al. 2001, 2003). Geisler et al. (2005), from high resolution spectroscopy of red giants, find $[\text{Fe}/\text{H}]$ values in the range from -2.10 to -0.97 dex, confirming a large metallicity spread in Sculptor. Two distinct ancient populations showing an abrupt change in the $[\text{Fe}/\text{H}]$ distribution at about 12 arcmin from the galaxy center are found in Sculptor by Tolstoy et al. (2004) based on FLAMES@VLT low resolution spectroscopy and WFI imaging of the galaxy. The two components have also different spatial distribution and velocity dispersion.

In this paper we present metal abundance determinations based on multi-slit low resolution spectroscopy obtained with FORS2 at the VLT for more than a hundred RR Lyrae stars in Sculptor. The variables are spread over a $15' \times 15'$ area around the galaxy centre, thus being almost coincident with the internal region of Sculptor where Tolstoy et al. (2004) find segregation of red HB stars. The knowledge of the *metal distribution* of the RR Lyrae population allows to put important constraints on the early star formation and chemical evolution histories of the host galaxy, by removing the age-metallicity degeneracy: the earliest measurable data point for the chemical enrichment history of Sculptor can be determined with accuracy.

Observations and data reduction are discussed in Section 2. Metal abundances are presented in Section 3. The

luminosity-metallicity relation and the radial velocities we determined for the RR Lyrae stars in Sculptor are discussed in Sections 4 and 5, respectively. In Section 6 the metallicity distribution of the Sculptor RR Lyrae stars is compared with that of other old stellar populations in the galaxy. A summary and some final remarks in Section 7 close the paper.

2 OBSERVATIONS AND DATA REDUCTIONS

Observations of 110 variable stars (107 RR Lyrae, 1 Anomalous Cepheid, 1 binary system, and 1 variable of unknown type) in Sculptor and of RR Lyrae stars in 4 Galactic globular clusters (namely: M 2, M 15, NGC 6171, and NGC 6441) were carried out using FORS2 (FOcal Reducer/low dispersion Spectrograph 2), mounted on the ESO Very Large Telescope (Paranal, Chile). The data were collected in service mode during the period July 29 to August 5, 2003. Typical seeing values during the observations were in the range $0''.7$ – $1''.7$ and on average of about $1''.2$. We used the MXU (Mask eXchange Unit) configuration, that allows to observe simultaneously many objects with more freedom in choosing the location, size and shape of individual slitlets with respect to the standard MOS mode. The detector is a mosaic of two MIT CCDs with $15 \mu\text{m}$ pixel size.

Spectra were collected using the blue grism GRIS_600B covering the 3450–5900 Å wavelength range, with a dispersion of 50 \AA mm^{-1} with slits $1''$ wide, and usually $14''$ long to allow for sky subtraction. With this configuration, each pixel corresponds to 0.75 \AA . An effort was made to cover for each star the relevant wavelength range (~ 3900 – 5100 \AA) containing both the CaII K and the hydrogen Balmer lines up to $\text{H}\beta$. We have used an instrumental set-up similar (i.e. same spectral range, resolution, and typical S/N) to that employed in our study of the RR Lyrae stars in the LMC (Gratton et al. 2004), so that RR Lyrae variables in some calibrating GCs are already available (namely in clusters NGC 1851, NGC 3201, and M 68). Exposure times on the Sculptor variables were of 31 min, as an optimal compromise between S/N and time resolution of the light curve of the RR Lyrae targets. We employed 9 masks in Sculptor, 2 in NGC 6441, 1 in M2, 1 in NGC 6171 and 1 in M15. The 9 Sculptor fields were slightly overlapped, so that for 25 variables we have more than 1 spectrum. A detailed log of the observations is given in Table 1 where N is the number of variable stars observed in each mask. The complete listing of the variables observed in Sculptor is provided in Table 2 where we have adopted Kaluzny et al. (1995) identification numbers. Their location on a $16' \times 16'$ map of the central region of Sculptor dSph galaxy is shown in Fig. 1. Finding charts corresponding to the nine $6.8' \times 6.8'$ FORS2 subfields are given in Appendix A. Centre of field coordinates are provided in Table 1. Equatorial coordinates for all our targets can be found in table 2 of Kaluzny et al. (1995).

Data reduction was performed using the standard IRAF¹ routines. Images have been trimmed, corrected for bias and for the normalized flat field. Then we used the

¹ IRAF is distributed by the NOAO, which are operated by AURA, under contract with NSF

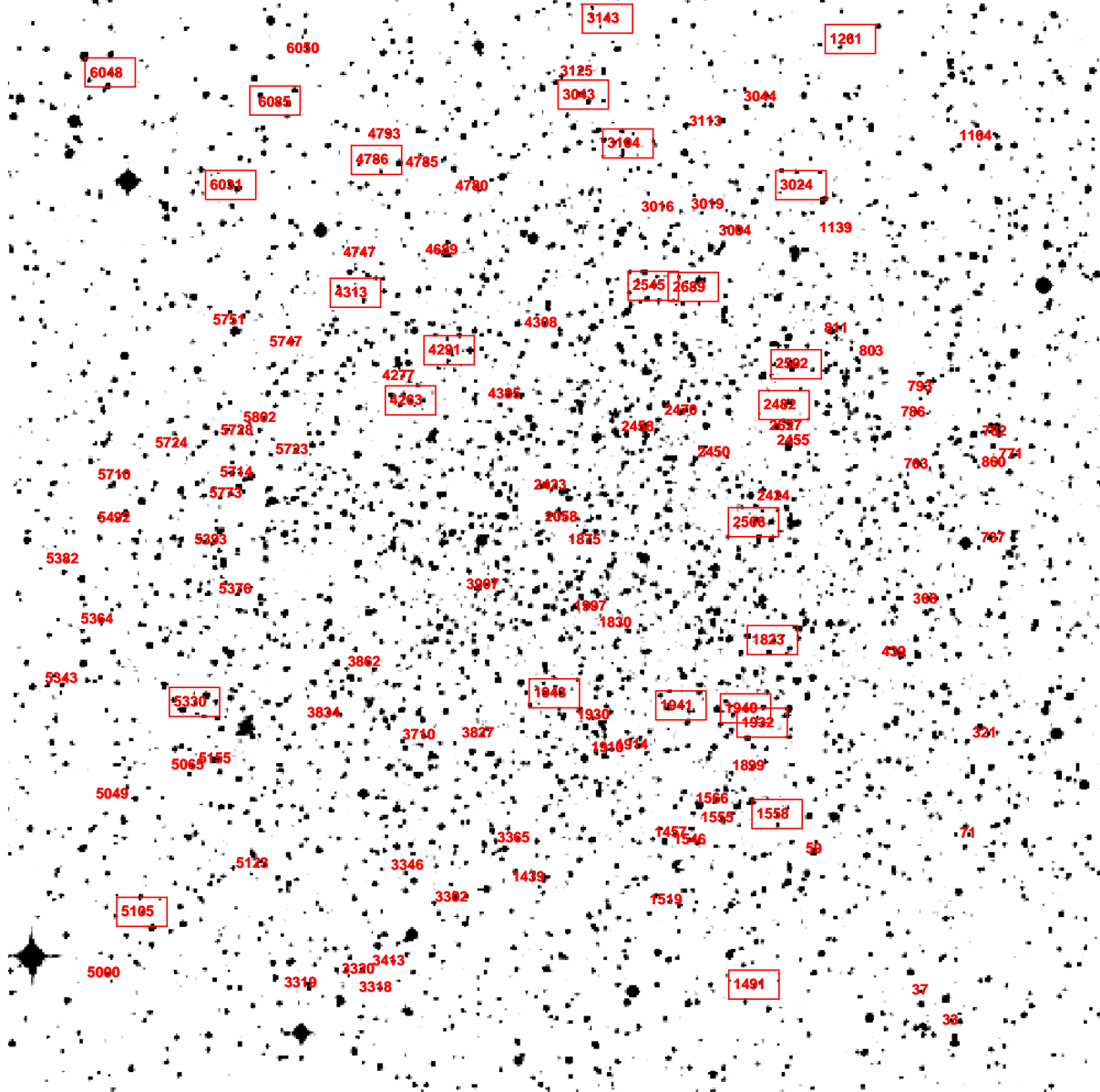


Figure 1. Position of the observed variables on a $16' \times 16'$ map of the centre of Sculptor dSph galaxy. North is up and East is to the left. Variables are identified according to Kaluzny et al. (1995) identifiers. Also shown (in blue in the electronic edition of the journal) are the four red giants recently analyzed by Geisler et al. (2005). Boxes mark the RR Lyrae stars for which we measured metallicities $[Fe/H] > -1.70$ dex (see Section 3.1).

IRAF command *lineclean* to reduce the contamination by cosmic rays. Up to 19 spectra were present in each pointing, and were extracted with the optimal extraction and automated cleaning options switched on. The sky contribution was subtracted making use of the slit length. The contamination of targets from nearby stars was reduced to a minimum, except for a few objects. For each science mask a HeCdHg lamp was acquired, and used to calibrate in wavelength the spectra, each one covering a different spectral range, depending on the target position. Not less than 10 lines of the calibration lamp were visible for each aperture, and the resulting dispersion solutions have r.m.s. of about 0.03 \AA . Further cleaning of cosmic rays hits and bad sky subtrac-

tions was done using the clipping option in the IRAF *splot* task. Fig. 2 shows examples of the final spectra.

3 DERIVATION OF THE METAL ABUNDANCES

We obtained spectra for 110 of the variable stars identified in Sculptor by Kaluzny et al. (1995), and for 25 of them we have multiple observations. These authors published photometry in the *V* band for all our targets. Periods and epochs of maximum light were determined from their time series data (kindly made available by Dr. J. Kaluzny), using the period search package GRaphical Analyzer of Time Series

Table 1. Log of the observations.

Field	RA (JD2000)	DEC (JD2000)	Date (UT)	Exptime (sec)	N
M15	21:30:13.4	12:11:50.4	2003-07-31	150	9
M2	21:33:40.4	-00:50:45.7	2003-08-05	150	6
NGC6171	16:32:34.6	-13:06:46.8	2003-07-29	150	6
NGC6441A	17:50:19.9	-37:05:21.9	2003-07-29	300	5
NGC6441B	17:50:24.5	-37:00:06.3	2003-07-30	300	7
SCL1	01:00:30.7	-33:38:18.4	2003-08-01	1860	15
SCL2	01:00:08.7	-33:38:18.5	2003-08-01	1860	18
SCL3	00:59:51.2	-33:38:18.5	2003-08-02	1860	15
SCL4	01:00:34.8	-33:42:43.1	2003-08-02	1860	15
SCL5	01:00:10.3	-33:42:43.5	2003-08-02	1860	19
SCL6	00:59:49.1	-33:42:45.0	2003-08-03	1860	18
SCL7	01:00:32.0	-33:47:18.5	2003-08-03	1860	15
SCL8	01:00:09.5	-33:47:15.5	2003-08-05	1860	19
SCL9	00:59:47.8	-33:47:53.8	2003-08-05	1860	13

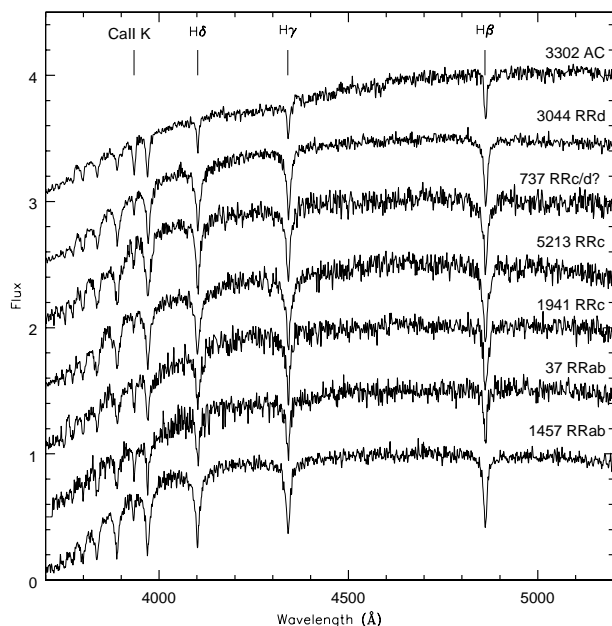


Figure 2. Examples of spectra of variable stars in Sculptor obtained using FORS2. The stars are identified according to Kaluzny et al. (1995). The six lower plots are RR Lyrae variables (from bottom to top: two fundamental mode, two first overtone, one suspected and one confirmed double-mode pulsator observed at different phases). The upper plot is an Anomalous Cepheid (star 3302). The spectra have been offset for clarity, and the main spectral lines are marked.

(GRATIS, Di Fabrizio 1999, Clementini et al. 2000). The new ephemerides are provided in Table 2. We found that our periods are in general slightly different from those published by Kaluzny et al. (1995); differences are in most cases around the fourth or fifth digit. However, there are a number of cases where our periods and type classifications significantly differ from those of Kaluzny et al. (1995) who published aliases of the periodicities preferred here. All these objects have been flagged in the last column of Table 2, where we provide comments on individual stars. We used

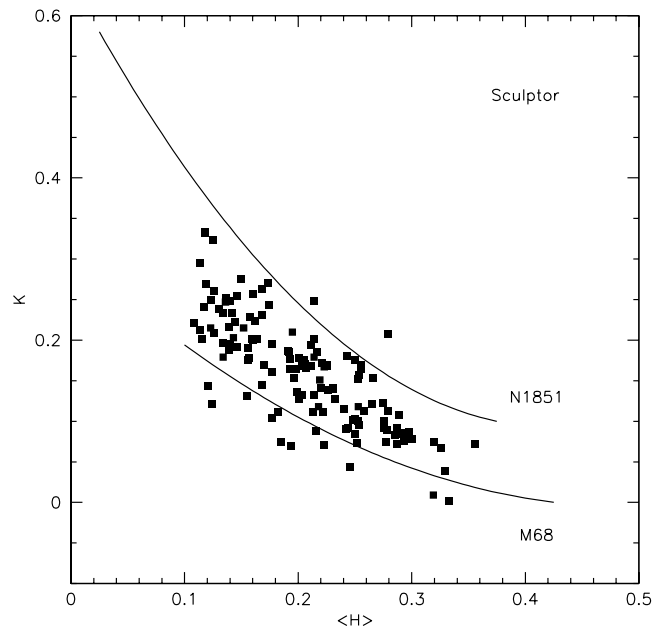


Figure 3. Correlation between K and $\langle H \rangle$ spectral indices for the variable stars in Sculptor. Solid lines represent the mean lines for M68 and NGC 1851 from Gratton et al. (2004).

our new periods to phase the spectra of our target stars in Sculptor since the scatter in the light curves appears to be significantly reduced than using the published values. Phases corresponding to the Heliocentric Julian Day (HJD) at half exposure are listed in Column 3 of Table 2; for the double-mode RR Lyrae stars they correspond to the first overtone pulsation period. We also computed intensity-averaged luminosities for all the variables in our study, that are given in Column 5 of Table 2. Based on our study of the light curves our sample contains 62 *ab*-type, 40 *c*-type, 3 confirmed and 2 suspected *d*-type RR Lyrae stars, 1 Anomalous Cepheid, 1 suspected binary system, and 1 variable of unknown type.

3.1 Metallicities and metal abundance distribution of the variable stars in Sculptor

Precise and homogeneous metal abundances for the target stars in Sculptor were measured using the revised version of the ΔS method (Preston 1959) devised by Gratton et al. (2004). We do not actually measure ΔS values, but rather estimate metallicities for individual variables by comparing the strength of the H lines and of the K Ca II line with analogous data for variables in GCs of known metallicity. A detailed description of our method can be found in Gratton et al. (2004). A summary of the technique, and an update of the calibration procedures are provided in Appendix B, to which the interested reader is referred to for details. Spectral line indices measured for the variables in Sculptor following Gratton et al. (2004), are given in Columns from 8 to 12 of Table 2. The correlation between K and $\langle H \rangle$ spectral indices is shown in Fig. 3. In this figure the solid lines represent the mean relations of the calibrating clusters M68 and NGC 1851 (see Appendix B). The variables in Sculptor fall almost entirely below the mean line of

NGC 1851 indicating that they are metal-poorer than this cluster ($[\text{Fe}/\text{H}]_{\text{ZW}} = -1.36$), and also extend below the mean line of M 68, showing that there is a number of variables in Sculptor metal-poorer than $[\text{Fe}/\text{H}]_{\text{ZW}} = -2.09$. Metallicity indices $M.I.$ defined according to equations (1), (2) and (3) in Appendix B, are listed in Column 13 of Table 2. Individual metallicities were derived from the calibration equations (4) and (5) in Appendix B in the Zinn & West (1984, hereafter ZW84) and in the Carretta & Gratton (1997, hereafter CG97) metallicity scales separately; they are listed in Columns 14 and 15 of Table 2. For different observations of the same star the $[\text{Fe}/\text{H}]$ values are averages of all the available measurements. From the objects with multiple observations we estimate that errors of individual abundance determinations are 0.15 and 0.16 dex in ZW84 and CG97 metallicity scales, respectively.

The average metal abundance of the 107 RR Lyrae stars in our sample is $[\text{Fe}/\text{H}] = -1.83 \pm 0.03$ (r.m.s. = 0.26 dex) with a total metallicity range of $-2.42 < [\text{Fe}/\text{H}] < -0.85$ in ZW84 scale, and an offset of about 0.2 dex to higher metallicity in CG97 scale. The star-to-star scatter inferred from the r.m.s. dispersions is about 0.19-0.23 dex, hence larger than typical measurement errors. If we adopt 0.23 dex as the measured metallicity spread, and quadratically subtract a $[\text{Fe}/\text{H}]$ measurement error of 0.16 dex, we obtain ~ 0.16 dex as our estimate of the intrinsic spread in the metal abundance of the Sculptor RR Lyrae stars.

The observed metallicity distribution of the Sculptor RR Lyrae stars (uncorrected for the measurement errors) in the ZW84 metallicity scale is shown in Fig. 4. Variable stars are divided by type. We find that the different types follow the same metallicity distributions. As well known, CG97 scale provides systematically higher metallicities than ZW84. In the following we will adopt ZW84 values, unless explicitly noted. However, independently of the adopted metallicity scale there are only very few metal-rich stars in our RR Lyrae sample. Based on the period distribution of the *ab*-type pulsators, Kaluzny et al. (1995) conclude that the bulk of the RR Lyrae stars in Sculptor have metallicities equal to or lower than $[\text{Fe}/\text{H}] = -1.7$. Indeed, there are only 26 stars with $[\text{Fe}/\text{H}] > -1.7$ in our sample. This is also the metallicity at which Tolstoy et al. (2004) find the break between metal-poor and metal-rich old populations in Sculptor. We will come back to this point in Section 6.

3.2 Comparison with metallicities from the Fourier parameters of the light curve and the pulsation equations

Metal abundances for the *ab*-type RR Lyrae stars in Sculptor have been estimated by Kovács (2001) using the parameters of the Fourier decomposition of the light curves and the Jurcsik & Kovács (1996) method. Derived metallicities are in the range from ~ -0.8 to -2.0 dex, with an average value of $[\text{Fe}/\text{H}] \sim -1.5$ dex in Jurcsik (1995) metallicity scale. Based on the frequency analysis of Kaluzny et al. (1995) data, Kovács (2001) also identified 15 confirmed and 3 suspected double mode pulsators in Sculptor and estimated their metal abundance using the pulsation equations. He found that, similarly to the RRab's, the bulk of the double-mode RR Lyrae stars in Sculptor have $[\text{Fe}/\text{H}] \sim -1.5$, with only two RRd's (stars 1168 and 5354 in Kaluzny et al. 1995)

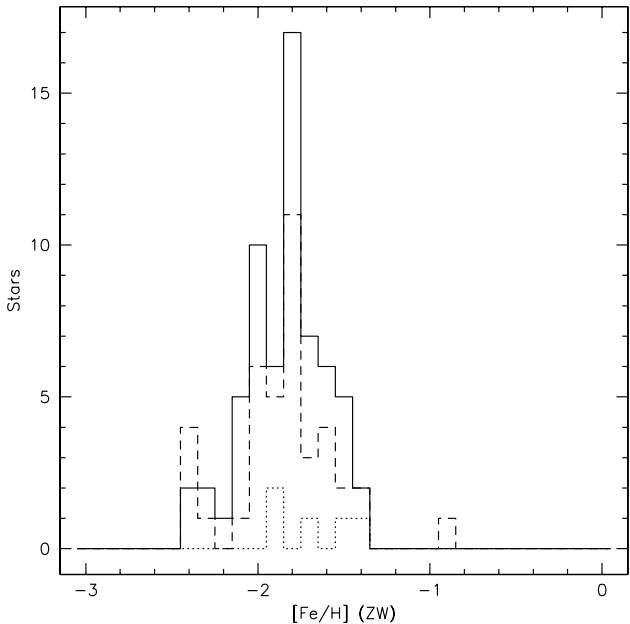


Figure 4. Metallicity distribution of the RR Lyrae stars in Sculptor using metal abundances in ZW84 metallicity scale. Variables are divided by type, solid line: RRab pulsators, dashed line: RRc pulsators, dotted line: RRd pulsators.

at $[\text{Fe}/\text{H}] = -1.9$. The metallicity distributions of RRab and RRd stars separately are shown in fig. 5 of Kovács (2001), and can be compared with our distribution in Fig. 4. We recall that the Jurcsik (1995) metallicity scale is on average 0.2 dex more metal rich than the ZW84 scale at $[\text{Fe}/\text{H}] \sim -1.5$. This partially accounts for the difference between average values in Kovács (2001) and in our distribution in Fig. 4, but there still is a residual difference of 0.17 dex between the average values, and our distribution appears to cover a metallicity range larger than in Kovács (2001).

We determined metallicities for six of the RRd variables discovered by Kovács (2001), three of which are actually only suspected RRd's. From our re-analysis of the light curves we think that these stars are monoperoic *c*-type RR Lyraes with noisy light curves. The comparison between individual metallicity values is shown in Table 3, where the range given in Column 4 was evaluated from the metallicity distribution of the RRd stars in fig. 5 of Kovács (2001). Unfortunately we did not observe the two most metal poor RRd's in Kovács (2001).

As with the RRab's the metallicity range spanned by the RRd stars we analyzed is larger than that obtained by Kovács (2001) for the same stars.

4 THE LUMINOSITY-METALLICITY RELATION

The luminosity-metallicity relation followed by the RR Lyrae stars in Sculptor was derived using the intensity-averaged mean magnitudes and the metal abundances in Table 2. We first discarded all objects that are not RR Lyrae stars or have incomplete light curves (stars 3302, 3710, 4780,

Table 2. Line indices and metal abundances of variable stars in Sculptor.

Star (a)	Type (b)	P (b)	Epoch (b)	$\langle V \rangle$ (b)	HJD (c)	ϕ	K	H_δ	H_γ	H_β	$\langle H \rangle$	$M.I.$	[Fe/H] ZW	[Fe/H] CG	V_r kms $^{-1}$	Notes
33	c	0.309071	9168.9087	20.110	6.7675	0.088	0.002	0.352	0.347	0.300	0.333	-0.280	-2.42	-2.26	89	
37	ab	0.508709	9162.9151	20.189	6.7675	0.230	0.161	0.168	0.199	0.164	0.177	0.239	-1.96	-1.78	68	
59	c	0.359681	9168.9359	20.176	6.7675	0.073	0.073	0.277	0.253	0.226	0.252	0.035	-2.14	-1.97	111	(d)
71	c	0.434922	9228.8270	20.015	6.7675	0.589	0.104	0.196	0.159	0.176	0.177	-0.127	-2.28	-2.12	105	
321	ab	0.601783	9167.9003	20.137	4.7959	0.616	0.234	0.120	0.133	0.148	0.134	0.386	-1.77	-1.57	101	
					6.7675	0.892	0.224	0.172	0.141	0.172	0.162	0.528			99	
368	c	0.358962	9184.8696	20.133	4.7959	0.727	0.096	0.269	0.249	0.245	0.254	0.252	-1.95	-1.76	108	
439	ab	0.496115	8809.6429	20.146	4.7959	0.658	0.215	0.141	0.161	0.152	0.152	0.401	-1.81	-1.62	109	
737	c/d?	0.338614	8809.8469	20.061	4.7959	0.612	0.083	0.308	0.294	0.252	0.285	0.328	-1.88	-1.69	96	(e)
763	c	0.293114	8830.8675	20.139	3.7485	0.615	0.128	0.280	0.239	0.176	0.232	0.370	-1.84	-1.65	102	
786	c	0.279088	8809.7457	20.179	3.7485	0.048	0.072	0.362	0.377	0.328	0.356	0.601	-1.64	-1.43	111	
793	c	0.359921	8809.9129	20.135	3.7485	0.339	0.118	0.268	0.264	0.228	0.253	0.442	-1.91	-1.72	107	
					4.7959	0.249	0.092	0.253	0.250	0.230	0.244	0.150			140	
803	ab	0.573658	8809.8060	20.061	3.7485	0.394	0.222	0.135	0.131	0.167	0.144	0.392	-1.82	-1.63	92	
811	c	0.363134	8809.8517	20.131	3.7485	0.098	0.092	0.308	0.283	0.268	0.287	0.420	-1.93	-1.75	131	
					4.7959	0.982	0.090	0.265	0.229	0.232	0.242	0.120			140	
860	c	0.359517	9158.9314	20.206	4.7959	0.071	0.140	0.299	0.208	0.185	0.231	0.464	-1.76	-1.56	129	(f)
1139	ab	0.518930	8809.5982	20.060	3.7485	0.245	0.075	0.299	0.262	0.269	0.277	0.194	-2.00	-1.82	127	
1164	ab	0.606190	8809.6323	20.185	3.7485	0.367	0.261	0.152	0.113	0.113	0.126	0.473	-1.75	-1.56	126	
1261	ab	0.630359	8809.4200	20.172	3.7485	0.912	0.323	0.106	0.134	0.137	0.125	0.782	-1.48	-1.26	148	
1439	c	0.356043	9168.9196	20.152	6.8001	0.952	0.115	0.292	0.230	0.199	0.240	0.324	-1.88	-1.70	104	(d)
1457	ab	0.717799	8827.8527	19.919	6.8001	0.915	0.085	0.341	0.295	0.243	0.293	0.398	-1.82	-1.63	74	
1491	c	0.357866	8809.7866	20.135	6.8001	0.727	0.153	0.350	0.225	0.223	0.266	0.854	-1.41	-1.20	84	(g)
1519	c	0.356859	9169.9083	20.173	6.7675	0.414	0.127	0.228	0.193	0.182	0.201	0.161	-2.03	-1.85	79	
1546	ab	0.531239	9174.9206	20.151	6.8001	0.737	0.143	0.076	0.158	0.129	0.121	-0.153	-2.31	-2.14	92	
1555	ab	0.527243	8823.8298	20.089	6.7675	0.112	0.078	0.312	0.301	0.286	0.300	0.372	-1.84	-1.65	81	
1558	c/d?/Bl	0.243016	8833.9116	20.203	6.8001	0.006	0.102	0.296	0.250	0.198	0.248	0.267	-1.65	-1.45	94	(h)
					6.7675	0.872	0.175	0.259	0.265	0.225	0.250	0.913			107	
1566	ab	0.570272	8809.9982	20.053	6.8001	0.266	0.177	0.175	0.210	0.193	0.193	0.458	-1.77	-1.57	107	
1823	c	0.298462	9189.8649	20.255	4.7959	0.373	0.152	0.294	0.230	0.235	0.253	0.743	-1.52	-1.30	107	
1830	ab	0.517855	8809.2712	20.224	3.8132	0.181	0.145	0.180	0.165	0.160	0.168	0.089	-2.09	-1.92	112	
1875	ab	0.499773	8823.9437	20.028	3.8132	0.400	0.188	0.153	0.151	0.113	0.139	0.174	-2.02	-1.84	95	(f)
1899	ab	0.646664	9182.9074	19.978	4.7959	0.201	0.071	0.240	0.219	0.210	0.223	-0.137	-2.29	-2.13	74	
1910	ab	0.572828	9189.9080	20.083	3.8132	0.172	0.111	0.183	0.185	0.177	0.182	-0.059	-2.11	-1.93	97	
					6.8001	0.386	0.209	0.133	0.128	0.118	0.126	0.208			77	
1914	ab	0.570540	8829.8781	20.220	6.8001	0.084	0.195	0.120	0.106	0.194	0.140	0.213	-1.87	-1.68	98	
					6.7675	0.027	0.248	0.137	0.133	0.138	0.136	0.478			78	
1930	ab	0.611160	9188.9162	20.251	3.8132	0.626	0.141	0.251	0.235	0.206	0.231	0.473	-1.79	-1.59	103	
					6.8001	0.514	0.165	0.220	0.170	0.190	0.193	0.380			119	(g)
1932	ab	0.506044	9174.9206	20.155	4.7959	0.848	0.275	0.143	0.152	0.155	0.150	0.731	-1.53	-1.32	118	
					6.8001	0.809	0.257	0.228	0.141	0.113	0.160	0.716			90	
1940	ab	0.692975	9224.7748	20.117	4.7959	0.312	0.332	0.127	0.137	0.091	0.118	0.769	-1.49	-1.28	98	
					6.7675	0.157	0.333	0.109	0.126	0.117	0.118	0.769			104	
1941	c	0.365674	9166.8670	20.152	6.7675	0.689	0.157	0.258	0.253	0.250	0.254	0.789	-1.47	-1.26	107	
1943	ab	0.551149	9169.9100	20.146	3.8132	0.045	0.203	0.172	0.131	0.127	0.143	0.281	-1.54	-1.32	89	
					6.8001	0.464	0.248	0.235	0.222	0.184	0.214	1.159			103	(i)
1997	ab	0.626766	8823.9437	20.136	3.8132	0.625	0.179	0.165	0.101	0.138	0.134	0.097	-2.08	-1.91	125	
2058	ab	0.503415	9226.9053	20.238	3.8132	0.610	0.133	0.224	0.212	0.204	0.214	0.288	-1.92	-1.73	96	
2423	c	0.358540	9167.9003	20.010	3.8132	0.328	0.202	0.170	0.149	0.157	0.159	0.372	-1.84	-1.65	120	(f)
2424	c	0.348780	8809.8058	20.145	4.7959	0.527	0.166	0.215	0.227	0.178	0.207	0.482	-1.75	-1.55	118	

and 5724). We also eliminated the most metal rich variable in our sample (star 4263), even if this star falls extremely well on the mean relations we derive. Following the procedure applied by Gratton et al. (2004) to the LMC RR Lyrae stars, we divided the Sculptor variables into 6 metallicity bins 0.1 dex wide; the corresponding average apparent magnitudes are given in Table 4 in the two metallicity scales,

respectively. A least square fit weighted by the errors in both variables gives:

$$\langle V \rangle = (0.092 \pm 0.027)([\text{Fe}/\text{H}]_{\text{ZW}} + 1.5) + (20.158 \pm 0.009)$$

where the errors in the slopes were evaluated via Monte Carlo simulations. The same slope is found for metallicities in CG97 scale.

The luminosity-metallicity relation of the Sculptor RR

Table 2. Cont.

Star (a)	Type (b)	P (b)	Epoch (b)	$\langle V \rangle$ (b)	HJD (c)	ϕ	K	H_δ	H_γ	H_β	$\langle H \rangle$	$M.I.$	[Fe/H] ZW	[Fe/H] CG	V_r kms $^{-1}$	Notes
2450	ab	0.617962	8810.1279	20.071	2.7656	0.886	0.252	0.141	0.141	0.126	0.136	0.500	-1.84	-1.65	113	
					3.8132	0.581	0.238	0.123	0.135	0.133	0.130	0.383		92		
					4.7959	0.172	0.192	0.136	0.157	0.146	0.146	0.239		108		
2455	ab	0.636250	9184.8700	20.156	3.7485	0.413	0.247	0.160	0.135	0.112	0.136	0.467	-1.76	-1.56	113	
					2458	c	0.357686	8809.6823	20.156	2.7656	0.446	0.118	0.260	0.208	0.187	0.218
					3.8132					0.375	0.201	0.228	0.208	0.205	0.214	0.802
2470	ab	0.693447	8809.4598	20.073	3.8132	0.245	0.168	0.183	0.220	0.207	0.203	0.467	-1.76	-1.56	94	
2482	c	0.365865	9167.8931	20.191	4.7959	0.233	0.108	0.337	0.250	0.279	0.289	0.600	-1.64	-1.44	135	(f)
2502	ab	0.487474	9185.8606	20.238	4.7959	0.419	0.123	0.268	0.300	0.258	0.275	0.645	-1.60	-1.39	140	(f)
2545	ab	0.674059	8809.0126	20.016	2.7656	0.104	0.168	0.224	0.231	0.220	0.225	0.644	-1.60	-1.39	116	
2566	ab	0.583517	9190.8800	20.234	4.7959	0.018	0.180	0.248	0.235	0.247	0.243	0.901	-1.38	-1.15	88	
2627	ab	0.575091	9166.8885	20.130	4.7959	0.733	0.192	0.136	0.157	0.146	0.146	0.239	-1.96	-1.78	108	
2689	ab	0.511352	8809.5668	20.139	3.7485	0.805	0.270	0.155	0.206	0.159	0.173	0.909	-1.37	-1.15	99	
3004	ab	0.715496	8809.5055	20.044	2.7656	0.990	0.187	0.199	0.183	0.192	0.191	0.514	-1.72	-1.52	129	
3016	c	0.360325	8809.8443	20.117	2.7656	0.220	0.139	0.279	0.227	0.172	0.226	0.414	-1.81	-1.61	131	(d)
3019	ab	0.732965	9162.9250	19.978	3.7485	0.472	0.202	0.112	0.094	0.138	0.115	0.109	-2.07	-1.90	105	
3024	ab/Bl?	0.572818	9223.7730	20.059	3.7485	0.052	0.179	0.197	0.229	0.216	0.214	0.641	-1.61	-1.40	143	(f)
3043	ab	0.623908	8810.0604	20.192	2.7656	0.650	0.178	0.201	0.199	0.204	0.201	0.529	-1.70	-1.50	129	
3044	d	0.354271	8810.0791	20.126	3.7485	0.044	0.092	0.319	0.283	0.227	0.276	0.355	-1.86	-1.67	133	(l)
3104	d	0.356984	8809.9225	20.209	2.7656	0.982	0.243	0.182	0.171	0.169	0.174	0.745	-1.51	-1.30	124	(l)
3113	ab	0.593260	8809.6681	20.098	2.7656	0.049	0.121	0.296	0.244	0.256	0.265	0.556	-1.79	-1.59	130	
					3.7485	0.706	0.216	0.152	0.134	0.130	0.139	0.319		116		
3125	ab	0.533130	8809.9264	20.120	2.7656	0.220	0.201	0.179	0.160	0.154	0.164	0.404	-1.81	-1.62	134	
3143	d	0.354531	9184.9270	20.188	2.7656	0.607	0.170	0.276	0.236	0.251	0.255	0.914	-1.36	-1.14	140	(l)
3302	AC	1.346056	9227.8700	18.560	4.8256	0.506	0.295	0.101	0.116	0.124	0.114	0.553	-1.78	-1.58	81	
					6.8001	0.975	0.089	0.289	0.294	0.251	0.278	0.340		84		
3318	ab	0.640243	9169.8898	20.148	4.8256	0.530	0.221	0.086	0.108	0.131	0.108	0.165	-2.02	-1.85	79	
3319	ab/Bl	0.564984	9223.8400	20.012	4.8256	0.703	0.229	0.172	0.148	0.153	0.158	0.524	-1.71	-1.51	89	
3320	c	0.282469	9192.9040	20.119	4.8256	0.954	0.067	0.341	0.338	0.300	0.326	0.403	-1.94	-1.76	84	
					6.8001	0.944	0.039	0.358	0.338	0.290	0.329	0.115		66		
3346	c	0.357547	9168.9247	20.125	4.8256	0.857	0.088	0.244	0.216	0.189	0.216	-0.043	-2.02	-1.84	96	
					6.8001	0.379	0.141	0.214	0.243	0.203	0.220	0.394		120		
3365	ab	0.668088	9235.8929	20.105	6.8001	0.807	0.196	0.126	0.157	0.119	0.134	0.187	-2.01	-1.82	99	
3413	c	0.359537	9167.9120	20.132	4.8256	0.607	0.194	0.247	0.206	0.181	0.211	0.727	-1.72	-1.52	90	
					6.8001	0.098	0.103	0.299	0.230	0.220	0.250	0.285		85		
3710	Bin?	0.473839	9192.9030	19.856	3.8132	0.070	0.046	0.215	0.205	0.182	0.201	-0.420	-2.56	-2.42	73	(f)
					4.8256	0.207	0.077	0.201	0.159	0.194	0.185	-0.270		85		
					6.8001	0.374	0.029	0.159	0.186	0.140	0.162	-0.646		89		
3827	ab	0.587708	9226.7339	20.135	6.8001	0.644	0.212	0.147	0.071	0.122	0.114	0.152	-2.04	-1.86	67	
3834	c	0.375237	9189.9150	20.003	3.7809	0.125	0.169	0.179	0.158	0.172	0.170	0.245	-1.84	-1.65	96	
					4.8256	0.909	0.164	0.204	0.205	0.184	0.198	0.400		85		
					6.8001	0.171	0.195	0.184	0.164	0.184	0.177	0.463		90		
3862	c	0.294092	9188.9188	20.219	3.7809	0.622	0.087	0.307	0.318	0.268	0.298	0.442	-1.78	-1.58	121	
3907	ab	0.583204	9169.9000	20.203	3.8132	0.683	0.269	0.126	0.093	0.137	0.119	0.464	-1.76	-1.56	112	
4263	c	0.284768	8820.7399	20.229	2.7333	0.861	0.208	0.284	0.283	0.268	0.279	1.493	-0.85	-0.60	111	
4277	c	0.306303	8809.7972	20.172	2.7333	0.136	0.113	0.332	0.254	0.251	0.279	0.576	-1.79	-1.60	115	
					3.8132	0.661	0.100	0.245	0.277	0.239	0.253	0.284		96		
4291	c	0.387992	8810.1654	20.057	2.7656	0.282	0.185	0.209	0.238	0.202	0.217	0.700	-1.64	-1.43	105	
					3.8132	0.982	0.186	0.206	0.191	0.180	0.192	0.514		106		
4308	c	0.358956	8809.7147	20.123	2.7656	0.364	0.112	0.229	0.240	0.170	0.213	0.122	-1.83	-1.64	118	
					3.8132	0.283	0.169	0.230	0.220	0.226	0.225	0.649		130		

Lyrae stars is shown in Fig. 5. It is based on 105 stars covering the metallicity range [Fe/H] from -1.36 to -2.42, and we used different symbols for the various types of RR Lyrae stars. All variables seem to follow the same luminosity-metallicity relation independent of type. Gratton et al. (2004) found that the LMC double-mode RR Lyrae stars are offset to brighter luminosities in the luminosity-metallicity plane and explain this evidence with the LMC RRd's being

more evolved than the single-mode pulsators. The lack of a similar difference in luminosity between single and double-mode Sculptor RR Lyrae stars suggests that in this galaxy also the single-mode variables are evolved.

A more striking difference is the slope of the luminosity-metallicity relation, significantly shallower than that ob-

Table 2. Cont.

Star (a)	Type (b)	P (b)	Epoch (b)	$\langle V \rangle$ (b)	HJD (c)	ϕ	K	H_δ	H_γ	H_β	$\langle H \rangle$	$M.I.$	[Fe/H] ZW	[Fe/H] CG	V_r kms ⁻¹	Notes
4313	ab	0.731064	8820.6952	20.111	2.7333	0.298	0.231	0.202	0.150	0.152	0.168	0.617	-1.63	-1.42	119	
4385	ab	0.487413	8809.8949	20.191	2.7656	0.550	0.200	0.108	0.190	0.183	0.160	0.376	-1.87	-1.68	117	
					3.8132	0.699	0.076	0.328	0.298	0.253	0.293	0.311			103	
4689	ab	0.639202	8809.9119	20.024	2.7656	0.843	0.178	0.150	0.137	0.183	0.157	0.221	-1.98	-1.79	108	
4747	ab	0.591979	9166.9255	20.181	2.7333	0.246	0.168	0.234	0.201	0.198	0.211	0.534	-1.70	-1.50	120	
4780	?	0.391270	8810.1007	19.958	2.7656	0.164	0.252	0.061	0.081	0.103	0.082	0.160	-2.03	-1.85	110	(m)
4785	ab	0.506109	8809.4911	20.139	2.7656	0.935	0.069	0.267	0.179	0.136	0.194	-0.283	-2.42	-2.27	63	
4786	ab	0.537290	9226.9054	20.102	2.7333	0.365	0.263	0.146	0.172	0.185	0.168	0.817	-1.45	-1.23	138	
4793	ab	0.559834	8809.1465	20.059	2.7333	0.839	0.131	0.163	0.158	0.142	0.155	-0.068	-2.23	-2.06	133	
5000	c	0.323261	9166.8850	20.158	4.8256	0.543	0.136	0.192	0.222	0.182	0.199	0.207	-1.99	-1.81	93	
5049	ab	0.648752	8825.8195	20.076	4.8256	0.392	0.234	0.151	0.115	0.160	0.142	0.444	-1.78	-1.58	96	
5065	c	0.380212	9222.7846	19.989	3.7809	0.931	0.101	0.322	0.275	0.231	0.276	0.440	-1.74	-1.54	125	
					4.8256	0.678	0.176	0.251	0.197	0.167	0.205	0.547			116	
5105	ab	0.556682	9166.8930	20.154	4.8256	0.847	0.255	0.162	0.108	0.168	0.146	0.588	-1.65	-1.45	132	
5123	c	0.325323	8810.9530	20.162	4.8256	0.327	0.074	0.325	0.323	0.312	0.320	0.441	-1.78	-1.59	95	
5155	ab	0.567457	8823.8298	20.090	4.8256	0.611	0.241	0.081	0.104	0.167	0.117	0.316	-1.89	-1.70	108	
5330	ab	0.645766	8809.3652	20.136	3.7809	0.976	0.210	0.170	0.202	0.214	0.195	0.704	-1.55	-1.34	110	(f)
5343	ab/Bl?	0.546964	9164.9231	20.181	4.8256	0.149	0.190	0.158	0.147	0.162	0.156	0.282	-1.92	-1.74	108	
5359	ab	0.670952	8809.7021	19.972	3.7809	0.375	0.121	0.108	0.115	0.150	0.124	-0.247	-2.39	-2.23	93	
5364	c	0.394203	9168.9185	19.943	3.7809	0.624	0.044	0.238	0.268	0.231	0.246	-0.248	-2.39	-2.23	135	(f)
5376	c	0.389520	9187.8882	20.079	3.7809	0.315	0.074	0.224	0.167	0.164	0.185	-0.287	-2.42	-2.27	137	
5382	ab	0.595937	9191.9233	20.171	3.7809	0.708	0.249	0.121	0.136	0.111	0.123	0.389	-1.83	-1.63	99	
5393	c	0.322741	9166.9255	20.081	3.7809	0.587	0.153	0.221	0.185	0.183	0.196	0.313	-1.89	-1.71	144	
5492	ab	0.528786	8833.9145	20.161	3.7809	0.065	0.171	0.222	0.205	0.190	0.206	0.515	-1.72	-1.52	115	
5710	c	0.355803	9227.7927	20.132	3.7809	0.997	0.133	0.234	0.205	0.171	0.203	0.219	-1.98	-1.79	141	
5714	c	0.292913	8809.7224	20.221	2.7333	0.747	0.113	0.267	0.280	0.228	0.258	0.434	-1.79	-1.59	84	
5723	ab	0.566020	9166.9255	20.250	2.7333	0.801	0.248	0.138	0.135	0.147	0.140	0.505	-1.73	-1.53	112	
5724	ab	0.498508	8809.8649	-	2.7333	0.400	0.009	0.326	0.333	0.298	0.319	-0.265	-2.40	-2.25	104	(f, n)
5747	ab	0.559848	8833.9264	20.040	2.7333	0.388	0.176	0.172	0.145	0.153	0.156	0.206	-1.99	-1.81	126	
5751	c	0.397328	8809.6162	20.083	2.7333	0.756	0.112	0.267	0.191	0.208	0.222	0.177	-1.99	-1.81	97	
					3.7809	0.393	0.072	0.340	0.276	0.245	0.287	0.233			118	
5773	ab	0.508760	8823.9310	20.223	3.7809	0.931	0.084	0.272	0.256	0.223	0.250	0.116	-2.07	-1.89	91	
5802	ab	0.514632	8810.9385	20.244	3.7809	0.788	0.215	0.107	0.121	0.142	0.123	0.221	-1.98	-1.79	150	
6031	c	0.326878	9168.9123	20.124	2.7333	0.709	0.172	0.244	0.216	0.203	0.221	0.637	-1.61	-1.40	140	(f)
6048	ab	0.626791	9224.8920	20.168	2.7333	0.964	0.167	0.229	0.221	0.220	0.223	0.623	-1.62	-1.41	117	
6050	c	0.305175	8809.7002	20.121	2.7333	0.227	0.151	0.248	0.228	0.180	0.219	0.462	-1.76	-1.57	139	
6085	c	0.361528	9235.7159	20.146	2.7333	0.808	0.165	0.293	0.243	0.228	0.255	0.869	-1.40	-1.18	139	

^a Identifiers are from Kaluzny et al. (1995)

^b Epochs are -2440000. Along with types, periods, and mean magnitudes (in intensity average) they were redetermined from the study of the light curves based on data from Kaluzny et al. (1995). In a number of cases (marked with notes) they differ significantly from values published in Kaluzny et al. (1995).

^c HJDs are -2452850, they correspond to the HJD at half exposure.

^d Kovács (2001) classifies star 59, 1439, and 3016 as suspected double-mode RR Lyrae stars, with periodicities of 0.35968/0.4837; 0.35604/0.47809; and 0.36033/0.48401 respectively. Our study of the light curves does not confirm these findings, we think these stars are monoperoiodic *c*-type variables with noisy light curves.

^e We think this is a double-mode RR Lyrae, we list the first overtone period.

^f Classification and periods differ significantly from Kaluzny et al. (1995) who published aliases of the periodicities preferred here.

^g Noisy spectrum.

^h We think this RR Lyrae could either be a double-mode or be affected by the Blazhko effect (Bl, Blazhko 1907).

ⁱ G band visible.

^l Kovács (2001) classifies these variables as double-mode RR Lyrae stars respectively with periodicities of 0.35427/0.47546 (3044), 0.35699/0.47975 (3104), and 0.35453/0.47630 (3143).

^m Variable star of unknown type.

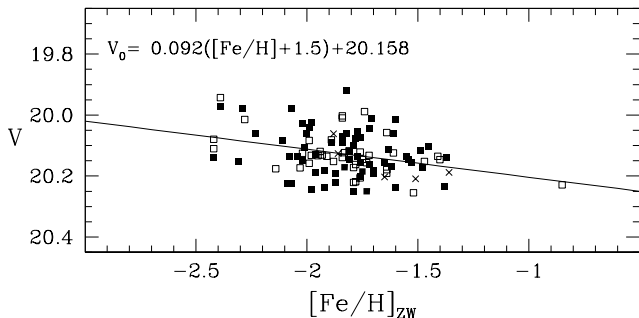
ⁿ Incomplete light curve.

Table 3. Comparison of the metallicities for RRd variable stars in Sculptor

Star	[Fe/H] _{this-paper} ZW84	[Fe/H] _{this-paper} CG97	[Fe/H] Kovács (2001)	Type Kovács (2001)	Type this paper
59	-2.14	-1.97	$-1.6 \leq [\text{Fe}/\text{H}] \leq -1.4$	RRd	RRc
1439	-1.88	-1.70	$-1.6 \leq [\text{Fe}/\text{H}] \leq -1.4$	RRd	RRc
3016	-1.81	-1.61	$-1.6 \leq [\text{Fe}/\text{H}] \leq -1.4$	RRd	RRc
3044	-1.86	-1.67	$-1.6 \leq [\text{Fe}/\text{H}] \leq -1.4$	RRd	RRd
3104	-1.51	-1.30	$-1.6 \leq [\text{Fe}/\text{H}] \leq -1.4$	RRd	RRd
3143	-1.36	-1.14	$-1.6 \leq [\text{Fe}/\text{H}] \leq -1.4$	RRd	RRd

Table 4. Metallicity distribution and average magnitudes of the RR Lyrae stars in Sculptor

[Fe/H] _{ZW} bin	n. stars	$\langle V \rangle$	$\langle [\text{Fe}/\text{H}]_{\text{ZW}} \rangle$	$\langle [\text{Fe}/\text{H}]_{\text{CG}} \rangle$
$[\text{Fe}/\text{H}] \leq -2.0$	22	20.093 ± 0.017	-2.175 ± 0.034	-2.005 ± 0.036
$-2.0 < [\text{Fe}/\text{H}] < -1.9$	14	20.139 ± 0.017	-1.957 ± 0.008	-1.773 ± 0.008
$-1.9 < [\text{Fe}/\text{H}] < -1.8$	19	20.099 ± 0.016	-1.846 ± 0.006	-1.656 ± 0.007
$-1.8 < [\text{Fe}/\text{H}] < -1.7$	23	20.140 ± 0.015	-1.757 ± 0.005	-1.559 ± 0.006
$-1.7 < [\text{Fe}/\text{H}] \leq -1.6$	13	20.144 ± 0.018	-1.638 ± 0.009	-1.432 ± 0.010
$-1.6 < [\text{Fe}/\text{H}]$	14	20.163 ± 0.012	-1.461 ± 0.018	-1.245 ± 0.019


Figure 5. Luminosity-metallicity relation of the RR Lyrae stars in Sculptor; variables are divided by type, filled squares: RRab pulsators, open squares: RRc pulsators, crosses: RRd pulsators.

tained for the LMC variables by Gratton et al. (2004)². On the other hand, we note that also the scatter in the average apparent luminosity of the RR Lyrae stars in Sculptor is less than half of that observed for the variables in the LMC: $\sigma_V(\text{Sculptor})=0.07$ mag, compared to the 0.15-0.16 mag in the LMC (Clementini et al. 2003b). This scatter is almost entirely accounted for by photometric errors and the dispersion in metallicity of the Sculptor RR Lyrae stars, thus indicating that these variables have a very similar degree of evolution off the zero age horizontal branch. The shallow slope of the luminosity-metallicity relation in Sculptor could thus be explained by the Sculptor RR Lyrae's being all rather evolved stars arising from the old metal poor population that also gives origin to the blue HB in the galaxy. Some support to this suggestion arises from the comparison

² However, we note that in both studies the slopes of the RR Lyrae luminosity-metallicity relations could be slightly underestimated by a few hundredths of magnitude, because of the relatively large errors of the individual $[\text{Fe}/\text{H}]$ values.

of the average luminosity of the RR Lyrae stars with that of non variable horizontal branch stars in Sculptor.

From the color-magnitude diagram of Sculptor, values of $\langle V_{\text{HB}} \rangle \simeq 20.18$ - 20.20 mag, $\langle V_{\text{blue HB}} \rangle \simeq 20.20$ and $\langle V_{\text{red HB}} \rangle \simeq 20.29$ mag are obtained by Kaluzny et al. (1995), Babusiaux, Gilmore, & Irwin (2005), and Rizzi (2003), respectively. This is at least $\simeq 0.06$ - 0.08 mag fainter than the average luminosity of the RR Lyrae stars which, for the 106 RR Lyrae with full light curve coverage, is $\langle V \rangle = 20.127$ with a dispersion of $\sigma = 0.072$ (this value agrees well with the estimate by Kaluzny et al. 1995, based on the total sample of 226 RR Lyrae stars in Sculptor).

5 RADIAL VELOCITY DETERMINATIONS

Radial velocities were measured from the spectra of the Sculptor RR Lyrae stars, and are given in Column 16 of Table 2. Multiple observations of the same stars show that our estimates have typical errors of about ± 15 km s⁻¹, with no systematic differences for different masks. This error includes the contribution of measurement uncertainties, errors related to the centering of the stars in the slit, and uncertainties due to the poor sampling of the radial velocity curves of the variable stars.

The average heliocentric radial velocity of all our variable stars in Sculptor is $\langle V_r \rangle = 109.1 \pm 1.9$ km s⁻¹ (r.m.s.=19.9 km s⁻¹, 110 stars, having preliminarily averaged individual values for stars with multiple observations). The average radial velocity of the RR Lyrae stars alone is $\langle V_r \rangle = 109.6 \pm 1.9$ km s⁻¹ (r.m.s.=19.8 km s⁻¹, 107 stars). These values are in excellent agreement with the estimate obtained from K-giants in Sculptor by Queloz, Dubath & Pasquini (1995: $\langle V_r \rangle = 109.9 \pm 1.4$ km s⁻¹) and are consistent with the value of $\langle V_r \rangle = 107 \pm 2.0$ km s⁻¹ previously derived by Armandroff & Da Costa (1986).

The good agreement with the literature values suggests that the offcentering problems noted for the calibrating cluster variables (see Appendix B) do not seem to af-

fect the variables in Sculptor and that the undersampling of the variable star's radial velocity curves does not significantly bias our estimates of the average V_r value. To further check this point we extracted from the database of the Galactic field RR Lyrae stars analyzed with the Baade-Wesselink method (Liu & Janes 1990; Jones et al. 1992; Cacciari, Clementini & Fernley 1992; Skillen et al. 1993; Fernley 1994) template radial velocity curves of *ab*- and *c*-type RR Lyrae stars with metal abundance comparable to that of the variable stars in Sculptor, and estimated phase-dependent radial velocity corrections for each spectrum of RR Lyrae star. Using this procedure we found that the average correction to apply to the radial velocity mean value of the 107 RR Lyrae stars in our sample is less than ~ 0.1 km s $^{-1}$ and can be safely neglected.

The difference between r.m.s. scatter of the RR Lyrae stars (19.8 km s $^{-1}$) and typical measurement errors (15 km s $^{-1}$) implies an intrinsic radial velocity dispersion of $\sigma=12.9$ km s $^{-1}$ for the RR Lyrae stars. This value is larger than the 6.3 ± 1.1 , -1.3 km s $^{-1}$ and 6.2 ± 1.1 km s $^{-1}$ found for the K-giants by Armandroff & Da Costa (1986) and Queloz et al. (1995), and for Sculptor metal rich red giant stars by Tolstoy et al. (2004; $\sigma_{metal-rich}=7 \pm 1$ km s $^{-1}$), but is consistent with the 11 ± 1 km s $^{-1}$ dispersion observed by these same authors for the metal poor red giants in Sculptor. This result gives further support to the hypothesis that the RR Lyrae stars in Sculptor arise from the old, metal-poor population giving origin to the galaxy blue-horizontal branch, although our value for their velocity dispersion needs to be confirmed by higher resolution spectroscopy.

6 METALLICITY DISTRIBUTIONS OF THE DIFFERENT OLD STELLAR COMPONENTS IN SCULPTOR

The average metallicity, metal abundance distribution and range in metal abundance spanned by the RR Lyrae stars can be compared with the analogous quantities for other old stellar components in Sculptor, namely with the metallicity spread inferred from the width of the red giant branch (e.g. Kaluzny et al. 1995; Majewski et al. 1999; Rizzi 2003; Babusiaux et al. 2005), and with the abundances directly measured for red giants in Sculptor by Geisler et al. (2005) and Tolstoy et al. (2004), respectively.

The metallicity distribution in Fig. 4 shows that the RR Lyrae stars in Sculptor cover a full metallicity range of about 1.6 dex, which however reduces to ~ 1 dex if the single most metal rich star in the sample is discarded. This range is larger than inferred from the spread of the red giant stars ($\Delta[\text{Fe}/\text{H}] \simeq 0.6$ dex, Kaluzny et al. 1995; Rizzi 2003; $\simeq 0.8$ dex, Majewski et al. 1999; $\simeq 0.7$ dex, Babusiaux et al. 2005), and is consistent with the spectroscopic study of red giants in Sculptor by Geisler et al. (2005: $\simeq 1.1$ dex) and Tolstoy et al. (2004) in the galaxy inner region (see upper panel of their fig. 3).

Tolstoy et al. (2004) find that the ancient stellar component (≥ 10 Gyr old) in Sculptor is divided into two distinct groups having different metal abundance, kinematics and spatial distribution. The metal-rich population is concentrated within the $r = 0.2$ degree central region, has metallicities in the range $-1.7 < [\text{Fe}/\text{H}] < -0.9$, ve-

locity dispersion of $\sigma_{metal-rich}=7 \pm 1$ km s $^{-1}$ and is related to the Sculptor red horizontal branch. The metal-poor population is more spatially extended, has metallicities in the range $-2.8 < [\text{Fe}/\text{H}] < -1.7$, velocity dispersion of $\sigma_{metal-poor}=11 \pm 1$ km s $^{-1}$ and is related to the Sculptor blue horizontal branch.

Our RR Lyrae stars are located in the central region of Sculptor, virtually coincident with the region where Tolstoy et al. (2004) find segregation of red HB stars. However, their metallicity distribution is dominated by the metal-poor objects with an average value of $[\text{Fe}/\text{H}]=-1.83$. The 26 stars with $[\text{Fe}/\text{H}] > -1.7$ are marked by boxes in Fig. 1. Their average luminosity $\langle V_{[\text{Fe}/\text{H}] > -1.7} \rangle = 20.154$ ($\sigma=0.060$, 26 stars) is marginally fainter than the average of the remaining 80 stars with $[\text{Fe}/\text{H}] \leq -1.7$ ($\langle V_{[\text{Fe}/\text{H}] \leq -1.7} \rangle = 20.118$, $\sigma=0.075$, 80 stars), as expected given the shallow slope of the Sculptor RR Lyrae luminosity-metallicity relation, and is anyway brighter than both the blue and red HBs of the non variable stars, thus indicating that they are evolved objects, like their metal-poor counterpart. The average radial velocity of the two samples is only marginally different: $\langle v_r \rangle = 117.5$ (r.m.s.=18.5, 26 stars) for the metal-rich sample and $\langle v_r \rangle = 107.0$ (r.m.s.=19.6, 80 stars) for the metal-poor stars. The r.m.s. scatters are very similar and, once deconvolved for the measurement errors (15 km s $^{-1}$), lead to very similar velocity dispersions of 10.8 and 12.6 km s $^{-1}$ in agreement with the velocity dispersion measured by Tolstoy et al. (2004) for the metal-poor component associated to Sculptor blue HB.

7 SUMMARY AND CONCLUSIONS

Low resolution spectra obtained with FORS2 at the VLT have been used to measure individual metal abundances $[\text{Fe}/\text{H}]$ and radial velocities for 107 RR Lyrae stars in the Sculptor dwarf spheroidal galaxy. Metallicities were derived using a revised version of the ΔS method (Gratton et al. 2004). The RR Lyrae stars in Sculptor are predominantly metal-poor with an average metal abundance of $[\text{Fe}/\text{H}]=-1.83 \pm 0.03$ (r.m.s.=0.26 dex) on the ZW84 metallicity scale, and only a few outliers having metallicities larger than -1.4 dex. The observed metallicity dispersion is larger than the observational errors, thus showing that these variables have a real metallicity spread.

The RR Lyrae stars in Sculptor are found to follow a luminosity-metallicity relation with a slope of 0.09 mag dex $^{-1}$, which is shallower than in the LMC (Gratton et al. 2004). This is explained with the Sculptor variable stars being rather evolved from the zero age HB, as also supported by their brighter luminosity compared to the non variable HB stars.

From our spectra we measured an intrinsic velocity dispersion 12.9 km s $^{-1}$ for the RR Lyrae stars, which appears to be in agreement with the dispersion derived by Tolstoy et al. (2004) for metal-poor red giants associated to the blue-HB stars in Sculptor.

All these evidences suggest that our RR Lyrae sample, and the RR Lyrae stars in Sculptor in general, are connected to the blue-HB population and arise from the first burst of star formation that produced the galaxy blue metal-poor HB. They allow to trace and distinguish this older compo-

ment in the internal regions of the galaxy which are otherwise dominated by the metal-rich and younger red-HB stars. Indeed, this component only produced a few, if any, of the Sculptor RR Lyrae stars since average luminosity and kinematic properties of the few metal-rich objects in our sample suggest that they are more likely the high metallicity tail of the metal-poor star population rather than objects associated with Sculptor red-HB stars.

ACKNOWLEDGMENTS

A special thanks goes to J. Kaluzny for providing us the time series photometry of the Sculptor variables. We thank the anonymous referee for his/her comments and suggestions. This research was funded by MIUR, under the scientific projects: 2002028935, “Stellar Populations in the Local Group” (P.I.: Monica Tosi) and 2003029437, “Continuity and Discontinuity in the Milky Way Formation” (P.I.: Raffaele Gratton).

REFERENCES

- Armandroff T.E., Da Costa G.S., 1986, *AJ*, 92, 777
 Babusiaux C., Gilmore G., Irwin M., 2005, *MNRAS*, 359, 985
 Bersier D., Wood P.R., 2002, *AJ*, 123, 840
 Cacciari C., Clementini G., Fernley J., 1992, *ApJ*, 396, 219
 Carretta E., Gratton R.G., 1997, *A&AS*, 121, 95
 Clement C.M., et al., 2001, *AJ*, 122, 2587
 Clement C.M., Shelton I., 1997, *AJ*, 113, 171
 Clementini G., et al. 2000, *AJ*, 120, 2054
 Clementini G., Gratton R.G., Bragaglia A., Carretta E., Di Fabrizio L., Maio M., 2003b, *AJ*, 125, 1309
 Clementini G., Gratton R.G., Bragaglia A., Ripepi V., Martinez Fiorenzano A.F., Held E.V., Carretta E., 2005, *ApJL*, in press (astro-ph/0508079)
 Clementini G., Held E.V., Baldacci L., Rizzi L., 2003a, *ApJ*, 588, L85
 Coutts C.M., Sawyer Hogg H., 1971, *Publ. David Dunlap Obs.* 3, 61
 Dolphin A.E., et al., 2001, *ApJ*, 550, 554
 Da Costa G.S., *ApJ*, 285, 483
 Di Fabrizio L. 1999, *Laurea Degree Thesis*, University of Bologna
 Fernley J., *A&A*, 284, L16
 Geisler D., Smith V.V., Wallerstein G., Gonzales G., Charbonnel C., 2005, *AJ*, 129, 1428
 Gratton R.G., Bragaglia A., Clementini G., Carretta E., Di Fabrizio L., Maio M., Taribello E., 2004, *AA*, 421, 937
 Harbeck D., et al., 2001, *AJ*, 122, 3092
 Held E.V., Clementini G., Rizzi L., Momany Y., Saviane I., Di Fabrizio L., 2001, *ApJ*, 562, L39
 Held E.V., Saviane I., Momany Y., Carraro G., 2000, *ApJ*, 530, L85
 Hurley-Keller D., Mateo M., Grebel E.K., 1999, *ApJ*, 523, L25
 Jones R.V., Carney B.W., Storm J., Latham D.W., 1992, *ApJ*, 386, 646
 Jurcsik J., 1995, *AcA*, 45, 653
 Jurcsik J., Kovács G., 1996, *AA*, 312, 111
 Lee J.-W., Carney B.W., 1999, *AJ*, 117, 2868
 Liu T., Janes K. A., 1990, *ApJ*, 354, 273
 Kaluzny J. Kubiak M., Szymański M., Udalski A., Krzemiński, Mateo M., 1995, *A&AS*, 112, 407
 Kovács G., 2001, *A&A*, 375, 469
 Majewski S., Siegel M.H., Patterson R.J., Rood R.T., 1999, *ApJ*, 520, L33
 Norris J., Bessell M.S., 1978, *ApJ*, 225, L49
 Preston G.W., 1959, *ApJ*, 130, 507
 Pritzl B.J., Armandroff T.E., Jacoby G.H., Da Costa G.S., 2002, *AJ*, 124, 1464
 Queloz D., Dubath P., Pasquini L., 1995, *A&A*, 300, 31
 Rizzi L. 2003, *Research Doctorate Thesis*, University of Padua
 Rizzi L., Held E. V., Bertelli G., Saviane I., 2004, *MmSAI*, 75, 110
 Siegel M., Majewski S., 2000, *AJ*, 120, 284
 Silbermann N.A., Smith H.A., 1995, *AJ*, 110, 704
 Skillen I., Fernley J., Stobie R.S., Jameson R.F., 1993, *MNRAS*, 265, 301
 Tolstoy E., Irwin M.J., Cole A.A., Pasquini L., Gilmozzi R., Gallagher J.S., 2001, *MNRAS*, 327, 918
 Tolstoy E., Venn K. A., Shetrone M., Primas F., Hill V., Kaufer A., Szeifert T., 2003, *AJ*, 125, 707
 Tolstoy E., et al., 2004, *ApJ*, 617, L119
 Zinn R., West M.J., 1984, *ApJS*, 55, 45

8 APPENDIX A - FINDING CHARTS

We present in this Section finding charts (Fig.s 6a,b,c) for all the variable stars we observed in Sculptor. They correspond to the nine $6.8' \times 6.8'$ FORS2 subfields used to map the central $15' \times 15'$ area of the galaxy. Centre of field coordinates are provided in Table 1. In each map North is up and East to the left, and variables are identified according to Kaluzny et al. (1995) identifiers. The RR Lyrae stars are marked by open circles (in red in the electronic edition of the journal), other types of variables by (blue) open squares. The complete listing of the variables observed in Sculptor is provided in Table 2. Equatorial coordinates for all our targets can be found in table 2 of Kaluzny et al. (1995).

9 APPENDIX B - THE METALLICITY CALIBRATION

Following the procedure devised by Gratton et al. (2004), line indices for RR Lyrae stars are computed from the spectra shifted to rest wavelength by directly integrating the instrumental fluxes in spectral bands centered on the Ca II K, H δ , H γ , and H β lines (see table 2 and fig. 10 of Gratton et al. 2004 for the definition of the spectral bands). Then a $\langle H \rangle$ index is defined as the average of the indices of the 3 hydrogen lines, and K as the index of the Ca II K line. Metallicities are derived by comparing the $\langle H \rangle$ and K indices measured for the target stars to the same quantities for variables in a number of globular clusters of known metal abundance.

The calibration of the line indices of the Sculptor variables in terms of metal abundances [Fe/H] was obtained using RR Lyrae stars in the newly observed clusters M15, M2 and NGC6171, and in the calibrating clusters

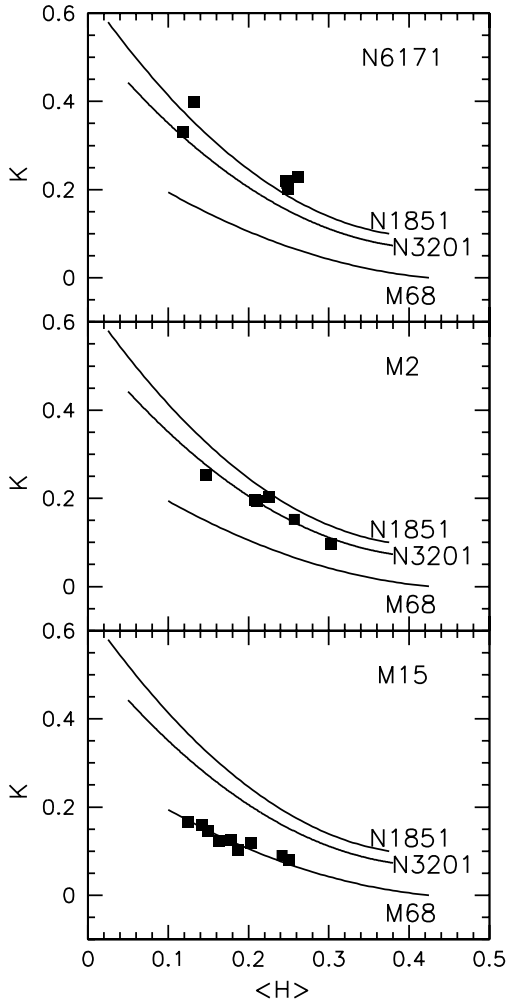


Figure 7. Correlation between K and $\langle H \rangle$ spectral indices for the calibrating clusters M15, M2, and NGC 6171 observed in the present run. Solid lines represent the mean lines for the calibrating clusters M68, NGC 3201, and NGC 1851, from Gratton et al. (2004).

used in Gratton et al. (2004), namely M68, NGC 1851 and NGC 3201. For all these clusters, precise metal abundances are available on both the ZW84 and CG97 metallicity scales. NGC 6441, a metal rich cluster ($[\text{Fe}/\text{H}] = -0.59$ according to ZW84 metallicity scale) having RR Lyrae stars with anomalously long periods, was not used for calibration purposes and will be discussed elsewhere (see Clementini et al. 2005).

Line indices measured for RR Lyrae stars in the calibrating clusters analyzed in the present paper are provided in Tables 5, 6, and 7 for M15, M2 and NGC 6171, respectively. The calibrating clusters define mono-metallic correlations in the K versus $\langle H \rangle$ plane. These relations are shown in Fig. 7 where filled squares represent stars in M15, M2 and NGC 6171, and solid lines are the mean relations defined by M68, NGC 1851 and NGC 3201 taken from Gratton et al. (2004). RR Lyrae stars in M15 fall precisely on the mean line of M68 and those in M2 closely follow the mean line of NGC 3201, confirming the good agreement between metal abundances of these two pairs of clusters. Stars in NGC 6171 generally fall slightly above the mean line of NGC 1851, in

agreement with the slightly higher metallicity of NGC 6171 with respect to NGC 1851.

According to Gratton et al. (2004) the mean relations drawn in Fig. 7 by M68 and NGC 1851 are:

$$K_1 = 0.3093 - 1.2815 \langle H \rangle + 1.3045 \langle H^2 \rangle \quad (1)$$

(valid for $\langle H \rangle$ between 0.12 and 0.40) for M68, and:

$$K_2 = 0.6432 - 2.6043 \langle H \rangle + 3.0820 \langle H^2 \rangle \quad (2)$$

(valid for $\langle H \rangle$ between 0.04 and 0.34) for NGC 1851. We thus defined metallicity index $M.I.$ the quantity:

$$M.I. = (K - K_1)/(K_2 - K_1) \quad (3)$$

where K is the Ca II K line index of the star, and K_1, K_2 are derived entering the $\langle H \rangle$ index measured for the star into equations (1) and (2). $M.I.$ values derived by this procedure for the RR Lyrae stars in the calibrating clusters analyzed in the present paper are listed in Column 10 Tables 5, 6, 7.

The calibration of the metallicity index in terms of metal abundance $[\text{Fe}/\text{H}]$ was derived by computing average $\langle M.I. \rangle$ values for the M15, M2 and NGC 6171 variables from the individual $M.I.$'s in Tables 5, 6, 7 and from the $M.I.$ values in Column 9 of tables 3, 4, and 5 of Gratton et al. (2004) for M68, NGC 1851 and NGC 3201, and correlating these $\langle M.I. \rangle$'s with the metal abundances of the clusters on the ZW and CG metallicity scales, respectively. The average $\langle M.I. \rangle$ values and their dispersions are summarized in Columns 6 and 7 of Table 8 along with the cluster metallicities (and their uncertainties) in the two metallicity scales (Columns from 2 to 5).

The correlation between $[\text{Fe}/\text{H}]$ and $\langle M.I. \rangle$ values is very well represented by linear regressions with scatter typically within the error of measure. These linear regressions are described by the following equations:

$$[\text{Fe}/\text{H}]_{\text{ZW}} = 0.882 \langle M.I. \rangle - 2.170 \quad (4)$$

$$[\text{Fe}/\text{H}]_{\text{CG}} = 0.941 \langle M.I. \rangle - 2.000 \quad (5)$$

and are shown in Fig. 8 for the ZW84 and CG97 metallicity scales, respectively.

Individual metal abundances for the RR Lyrae stars in the calibrating clusters analyzed in the present paper were derived from the above calibration equations. They are listed in Tables 5, 6, 7 respectively, while the mean metallicities derived from the averages of these individual values and their respective dispersions are given in Table 8.

The last column in each of Tables 5, 6, and 7 gives individual radial velocities measured from the spectra of the stars observed in the calibrating clusters. Averages of these values are listed in Table 8. We note that these average radial velocities differ somewhat from the literature values, particularly for NGC 6171, suggesting the presence of systematic offsets possibly caused by offcentering of the cluster variables in the slit. These systematic differences are not found in the case of the Sculptor variables, for which the average radial velocity we measured is perfectly consistent with the literature values (see Section 5). This suggests that we are simply seeing an effect of the small samples in the Galactic clusters, while the one in Sculptor is large enough to average away the offcentering effects.

Table 5. Line indices and metal abundances of RR Lyrae stars in the globular cluster M 15

M15												
Star (a)	HJD (-2400000)	Type	ϕ (b)	K	H_δ	H_γ	H_β	$\langle H \rangle$	$M.I.$	[Fe/H] ZW	[Fe/H] CG	V_r kms ⁻¹
V10	52851.6744	c	0.781	0.126	0.195	0.192	0.147	0.178	0.025	-2.15	-1.98	-83
V12	52851.6744	ab	0.645	0.159	0.148	0.155	0.122	0.142	0.027	-2.15	-1.98	-92
V17	52851.6744	d	0.429	0.123	0.181	0.151	0.158	0.163	-0.073	-2.23	-2.07	-96
V19	52851.6744	ab	0.592	0.090	0.272	0.247	0.208	0.242	0.121	-2.06	-1.89	-122
V23	52851.6744	ab	0.024	0.118	0.218	0.208	0.184	0.203	0.108	-2.08	-1.90	-118
V25	52851.6744	ab	0.492	0.167	0.141	0.107	0.126	0.125	-0.015	-2.18	-2.01	-99
V29	52851.6744	ab	0.967	0.146	0.170	0.145	0.133	0.149	-0.002	-2.17	-2.00	-114
V42	52851.6744	c	0.818	0.102	0.228	0.171	0.163	0.187	-0.092	-2.25	-2.09	-99
V50	52851.6744	c	0.298	0.079	0.272	0.253	0.225	0.250	0.078	-2.10	-1.93	-104

^a Star identifiers are from Sawyer-Hogg on line catalogue of variable stars in Galactic globular clusters published by Clement et al. (2001)

^b Phases were calculated from the HJD of observation using epochs and periods corrected according to the rates of period changes published by Silbermann & Smith (1995).

Table 6. Line indices and metal abundances of RR Lyrae stars in the globular cluster M 2

M2												
Star (a)	HJD (-2400000)	Type	ϕ (b)	K	H_δ	H_γ	H_β	$\langle H \rangle$	$M.I.$	[Fe/H] ZW	[Fe/H] CG	V_r kms ⁻¹
V10	52856.7503	ab	0.758	0.194	0.221	0.219	0.193	0.211	0.722	-1.53	-1.32	-38
V15	52856.7503	c/d	0.345	0.097	0.319	0.308	0.281	0.303	0.583	-1.66	-1.45	-25
V26 ^c	52856.7503	c	0.428	0.196	0.224	0.223	0.177	0.208	0.716	-1.54	-1.33	-21
V32 ^c	52856.7503	c	0.350	0.152	0.266	0.257	0.249	0.257	0.774	-1.49	-1.27	-34
V7	52856.7503	ab	0.621	0.203	0.221	0.217	0.238	0.225	0.923	-1.36	-1.13	-36
V3 ^d	52856.7503	ab	0.191	0.253	0.150	0.144	0.147	0.147	0.585	-1.65	-1.45	-15

^a Star identifiers are from Sawyer-Hogg on line catalogue of variable stars in Galactic globular clusters published by Clement et al. (2001)

^b Phases of the spectra were derived from the HJD of observation and the ephemerides published by Lee & Carney (1999).

^c Variable stars V26 and V32 correspond to stars LC608 and LC864 of Lee & Carney (1999), respectively.

^d Doubtful identification.

Table 7. Line indices and metal abundances of RR Lyrae stars in the globular cluster NGC 6171

NGC 6171												
Star (a)	HJD (-2400000)	Type	ϕ (b)	K	H_δ	H_γ	H_β	$\langle H \rangle$	$M.I.$	[Fe/H] ZW	[Fe/H] CG	V_r kms ⁻¹
V2	52849.5952	ab	0.746	0.330	0.113	0.128	0.117	0.119	0.771	-1.49	-1.27	-77
V4	52849.5952	c	0.385	0.220	0.283	0.241	0.219	0.247	1.280	-1.04	-0.80	-91
V6	52849.5952	c	0.570	0.214	0.256	0.284	0.205	0.248	1.239	-1.08	-0.83	-87
V7	52849.5952	ab	0.683	0.399	0.124	0.129	0.142	0.132	1.234	-1.08	-0.84	-86
V9	52849.5952	c	0.793	0.201	0.277	0.238	0.231	0.249	1.133	-1.17	-0.93	-96
V21	52849.5952	c	0.774	0.228	0.267	0.295	0.222	0.262	1.504	-0.84	-0.59	-77

^a Star identifiers are from Sawyer-Hogg on line catalogue of variable stars in Galactic globular clusters published by Clement et al. (2001)

^b Phases were derived from the HJD of observation, the periods published by Clement & Shelton (1997) and the epochs we estimated from the study of the light curves published from the same authors. V2 was not observed by Clement & Shelton (1997), for this star the adopted ephemerides, from Coutts & Sawyer Hogg (1971), may be no longer valid.

Table 8. Calibration of the metallicity index

Cluster	[Fe/H] ZW	err	[Fe/H] CG	err	$\langle M.I. \rangle$	err	$\langle [\text{Fe}/\text{H}] \rangle$ This paper ZW scale	σ	$\langle [\text{Fe}/\text{H}] \rangle$ This paper CG scale	σ	$\langle V_r \rangle$ km s ⁻¹
NGC 1851	-1.36	0.09	-1.03	0.06	1.007	0.028	-1.36 ± 0.02^a	0.10	—	—	—
NGC 3201	-1.61	0.12	-1.24	0.03	0.710	0.030	-1.56 ± 0.02^a	0.08	—	—	—
NGC 4590 (M68)	-2.09	0.11	-2.00	0.03	0.000	0.014	-2.09 ± 0.01^a	0.05	—	—	—
NGC 6171	-0.99	0.06	-0.95	0.04	1.194	0.098	-1.12 ± 0.09	0.21	-0.88 ± 0.09	0.22	-86 ± 3
NGC 7078 (M15)	-2.15	0.08	-2.02	0.04	0.020	0.025	-2.15 ± 0.02	0.06	-1.98 ± 0.02	0.07	-103 ± 4
NGC 7089 (M2)	-1.62	0.07	-1.31	0.04	0.717	0.052	-1.54 ± 0.05	0.11	-1.33 ± 0.05	0.12	-28 ± 4

^a Averages of the values in tables 3,4, and 5 of Gratton et al. (2004) corrected downward respectively by 0.10, 0.07 and 0.03 dex to account for systematic differences between ZW84 and the metallicity scale adopted in Gratton et al. (2004).

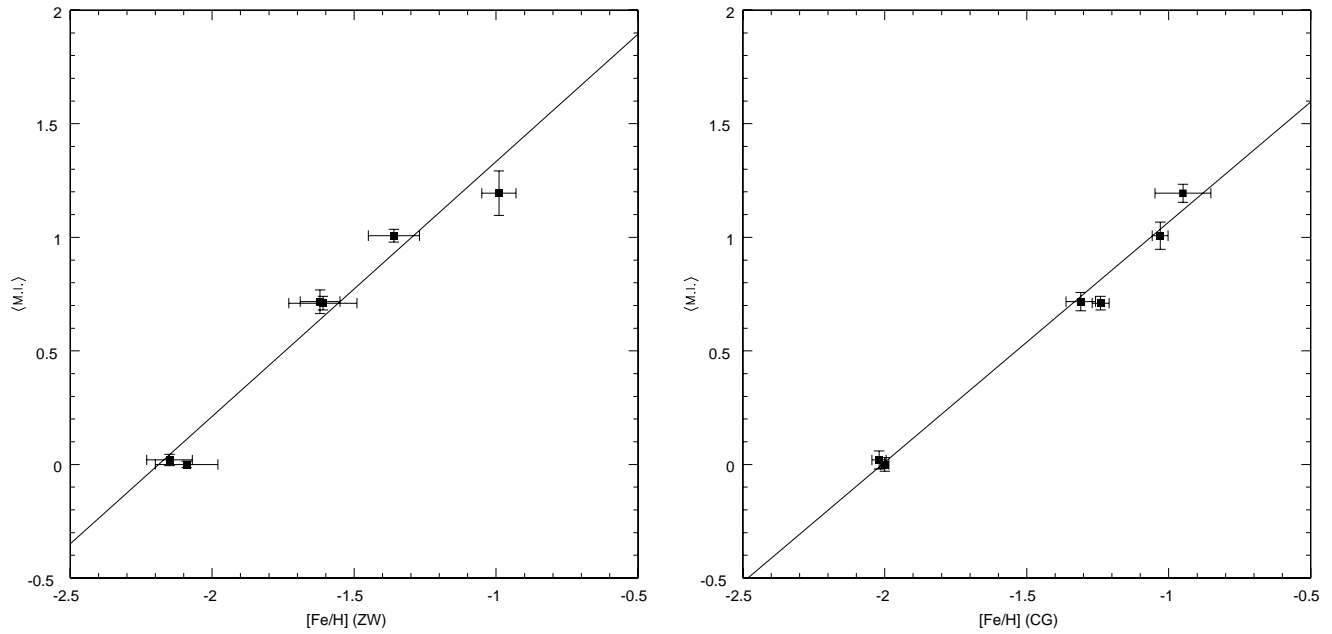


Figure 8. Calibration of the metallicity index (M.I.) on ZW84 (left panel), and CG97 (right panel) metallicity scales.

This figure "MF448fig6a.jpg" is available in "jpg" format from:

<http://arxiv.org/ps/astro-ph/0506206v2>

This figure "MF448fig6b.jpg" is available in "jpg" format from:

<http://arxiv.org/ps/astro-ph/0506206v2>

This figure "MF448fig6c.jpg" is available in "jpg" format from:

<http://arxiv.org/ps/astro-ph/0506206v2>

This figure "MF448fig6d.jpg" is available in "jpg" format from:

<http://arxiv.org/ps/astro-ph/0506206v2>

This figure "MF448fig6e.jpg" is available in "jpg" format from:

<http://arxiv.org/ps/astro-ph/0506206v2>

This figure "MF448fig6f.jpg" is available in "jpg" format from:

<http://arxiv.org/ps/astro-ph/0506206v2>

This figure "MF448fig6g.jpg" is available in "jpg" format from:

<http://arxiv.org/ps/astro-ph/0506206v2>

This figure "MF448fig6h.jpg" is available in "jpg" format from:

<http://arxiv.org/ps/astro-ph/0506206v2>

This figure "MF448fig6i.jpg" is available in "jpg" format from:

<http://arxiv.org/ps/astro-ph/0506206v2>